

HUMAN RESPIRATORY CONTROL SYSTEM: DYNAMICS AND STABILITY ANALYSIS

J. J. Batzel* H. T. Tran[†]

September 5, 2001

Abstract

Since 1940 a number of mathematical models of the human respiratory control system have been developed to study a wide range of features of this complex system. Among them, periodic breathing (including Cheyne-Stokes respiration and apneustic breathing) is a collection of regular but involuntary breathing patterns that have important medical implications. The purpose of this paper is to study the stability characteristics of a nonlinear system of five differential equations with multiple delays in both the state and control variables for modeling human respiration. Numerical simulations were performed to study instabilities in the human respiratory control system including the occurrence of periodic breathing and to test the hypothesis that periodic breathing is the result of delay in the feedback signals to the respiratory control system.

1 Introduction

The purpose of the respiratory system is to exchange the unwanted gas byproducts of metabolism, such as CO_2 , for O_2 , which is necessary for metabolism. The site of this exchange is the alveoli, small bubble-like sacs which are found in the lungs. There are approximately 300 million alveoli with a roughly spherical shape and a diameter of .3 mm. The alveoli represent a surface area of 50 to 100 square meters, by far the largest surface area of the body interfacing with the environment. Amazingly, this surface area encompasses a volume of

*SFB Optimierung und Kontrolle, University of Graz, Heinrichstrabe 22, A-8010 Graz (Austria), (jjbatzel@tom.kfunigraz.ac.at).

[†]Center for Research in Scientific Computation and, Department of Mathematics, Box 8205, North Carolina State University, Raleigh, North Carolina, 27695-8205, (tran@control.math.ncsu.edu).

only four liters. Intertwined among the alveoli are the smallest level of blood vessel, the capillaries. The capillaries form a dense network of tubes 10 microns in diameter in the walls of the alveoli resulting in an extremely thin blood-gas barrier. Mixed venous blood collected in the right ventricle of the heart is pumped into the pulmonary artery which branches successively, terminating in the capillaries. Each red blood cell spends approximately one second passing through two to three alveoli. The gas exchange boundary is so efficient that this is all the time needed for the red blood cells to completely exchange CO_2 for O_2 by passive diffusion. The blood is then collected back in the pulmonary veins and returned to the left auricle and then to the left ventricle where the blood is pumped to the systemic circulatory system.

Gas exchange is accomplished solely by passive diffusion of gases across the blood/gas barrier between capillaries and alveoli. The primary determiner of diffusion is the partial pressure gradients across this barrier. O_2 diffuses into the capillaries and CO_2 into the alveoli. O_2 is carried in the red blood cell both in a simple dissolve state and bound to hemoglobin which increases the efficiency of absorption and storage. CO_2 is carried in three different ways by the blood but, being twenty times more soluble than O_2 , the simple dissolved state is more significant for CO_2 . For efficient gas exchange, it is important that blood flow rate and ventilation (air flow) rate be matched within the various regions of the lung. For comprehensive references on respiratory physiology, see, for example, [14, 19].

The control mechanism which responds to the changing needs of the body to acquire oxygen and expel CO_2 acts to maintain the levels of these gases within very narrow limits (and to a less understood degree match ventilation and blood flow). The means by which this is accomplished is fairly well understood and consists of three components: (i) sensors which gather information; (ii) effectors which are nerve/muscle groups which control ventilation; and (iii) the control processor located in the brain which organizes information and sends commands to the effectors. The sensory system consists of two main components: the central sensors and the peripheral sensors; see Figure 1.

Since the control processor response to the central and peripheral sensor information is additive it is common practice to refer to the peripheral sensory system as the peripheral control and the central sensory system as the central control. The central sensors are found in the medulla area of the brain and respond to the level of CO_2 partial pressure (and to pH levels as well, though the mechanism is not well understood [19]). CO_2 partial pressure is the main factor stimulating ventilation [6]. The peripheral chemoreceptors are found in the carotid bodies located at the bifurcation of the common carotid arteries and

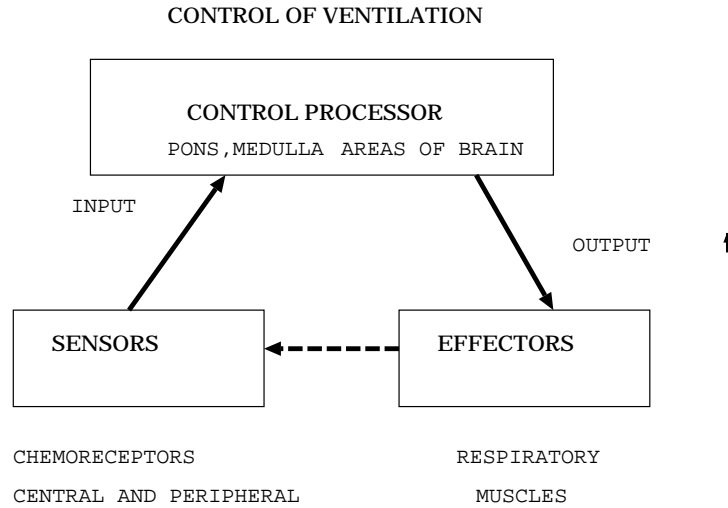


Figure 1: Schematic diagram of the human respiratory control system.

the aortic bodies above and below the aortic arch [6]. These receptors respond to both O_2 partial pressures and CO_2 partial pressures. The carotid bodies also respond to pH levels and are much more important than the aortic bodies in respiratory control. Both the aortic and carotid bodies act to regulate the cardiovascular system as well [14]. The response of the peripheral receptors is swift due to the relatively high blood flow through the carotid bodies. The peripheral response to CO_2 accounts for only 20-25 % of the overall response due to CO_2 partial pressure. The other 75-80 % is due to the central receptors [19]. There are differences in the response profiles of peripheral and central receptors to CO_2 and O_2 levels resulting in a highly intricate set of possible response signals to the myriad of possible levels of CO_2 and O_2 . The control system can thus respond successfully to a wide range of conditions. The sensitivity of this control is such that, regardless of the variation in the daily levels of rest and activity, the CO_2 partial pressure remains within 3 mm of its normal level of 40 mm Hg [19].

2 Periodic Breathing

Periodic breathing (PB) is the generic name given to a number of breathing patterns which are involuntary and have a regular pattern. The most impor-

tant forms of PB [8] are: (i) Cheyne-Stokes breathing which is illustrated in Figure 2; (ii) apneustic breathing; and (iii) Biots breathing. Periodic breathing patterns are aberrations in normal breathing patterns and can have important medical implications. Among them, patients with brain stem lesions, patients with congestive heart problems, normal individuals during sleep and at high altitudes, and newborn infants (which may be related to SIDS).

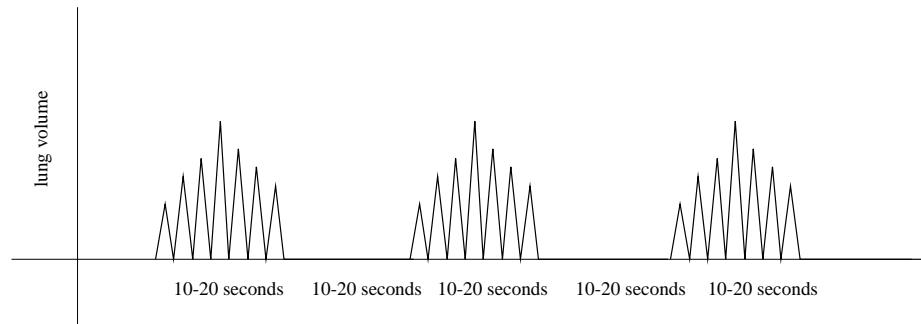


Figure 2: Cheyne-Stokes respiration.

A number of causes for PB have been proposed, including cardiovascular and neurological causes [8]. Perhaps the most widely held theory, introduced by Haldane and Douglas in 1909 [4], holds that PB is caused by instability in the respiratory control system. It appears that PB is mediated by the peripheral sensory mechanism and is effected by the delay in the feedback control loop. Significant delay in the feedback loop can result in the system reacting to information which no longer describes the state of the system. This can result in the so called “hunting phenomenon” where the system control incorrectly adjusts the control response to stabilize a state which no longer obtains. Excessive or diminished controller gain also affects feedback effectiveness. Considered as a dynamical system with delay, well known mathematical results such as given in [2] show that long delay times in the feedback control loop will destabilize a system and produce oscillations.

Studies done to vary peripheral controller gain and feedback delay support this [8, 9]. In particular, see [13], stability can be affected by circulation delay times, central and peripheral control gain, hypoxia and control response to hypoxia, and sleep/arousal state. The respiratory control system mechanism acts by means of negative feedback. Deviations in blood gas levels from physiological set points induce changes in ventilation rates which tend to compensate for these deviations. As mentioned above, the amount of blood flow to the

peripheral sensors is extraordinary and thus medical problems restricting this flow may also be a cause for instability.

The sensory mechanisms and the effector organs are separated by a physical distance and thereby introduce transport delays into the control system (see Figure 1). Corrective adjustments to ventilation will be thus delayed and together with changes in controller gain may lead to damped or sustained oscillations in the control system. Modeling studies have been done to test this hypothesis [11]. Apnea (lack of ventilation) can occur when the oscillations in the ventilatory control signal drive the signal to the cutoff point. Apnea has been associated with the phenomenon of Sudden Infant Death Syndrome (SIDS) and thus a fuller understanding of mechanisms producing it is important [18, 1].

3 A Mathematical Model for the Respiratory Control System

In this section we briefly describe the mathematical model developed in [11] and later was extended in [1] for modeling human respiration. The following standard symbol sets will be used throughout the paper.

Primary Symbols:

M = maximum effective volume in compartment,

MR = metabolic rate,

P = partial pressure,

Q = volume of blood,

\dot{Q} = volume of blood per unit time,

τ = delay,

\dot{V} = volume of gas per unit time.

Secondary Symbols for the Gas Phase:

A = alveolar,

AT = sea level air pressure,

B = brain,

C = carbon,

D = dead space,

E = expired,

I = inspired,

L = lung,

O = oxygen,

T = tissue.

Secondary Symbols for the Blood Phase:

a = mixed arterial,

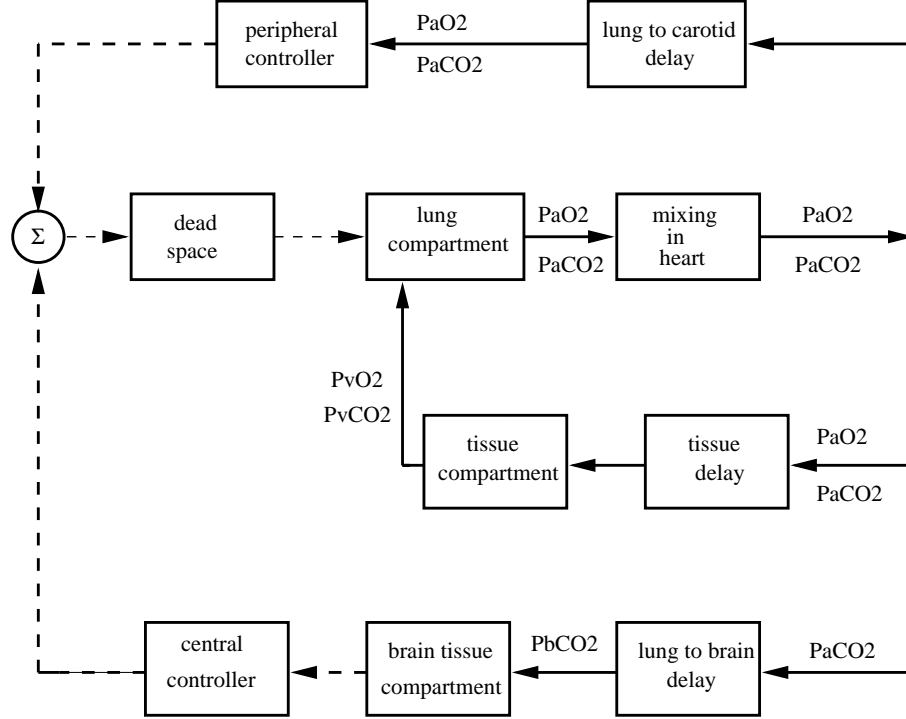
c = capillary,

\hat{c} = end-capillary,

i = ideal,

v = mixed venous.

For example, P_{aO_2} indicates arterial partial pressure of O_2 leaving the lungs and \dot{V}_I represents the inspired ventilation rate. The equations for the model studied arise from straightforward development of mass balance equations utilizing Fick's law, Boyle's law and variations of Henry's law relating the concentration of a gas in the solution to the partial pressure of the gas interfacing with the solution. The model describes three compartments: the lung compartment, a general tissue compartment and a brain compartment. A block diagram describing the the relationships between the three compartments and transport delays is shown in Figure 3. Delay is introduced into the respiratory control system due to the physical distance which CO_2 and O_2 levels must be transported to the sensory sites before the ventilatory response can be adjusted. Moreover, the delay times are state dependent since they depend on cardiac output in general and blood flow rate to the brain in particular. Basic models, which describe cardiac output and cerebral blood flow rates in terms of P_{aCO_2} , P_{aO_2} , and levels of CO_2 and O_2 in the brain respectively, can be found in [1]. In the following representation, the transport delays are denoted by: τ_B = lung to brain delay, τ_T = lung to tissue transport delay, τ_V = venous side transport delay from tissue to lung, and τ_a = lung to carotid artery delay.



MODEL SCHEMATIC DIAGRAM WITH DELAYS

Figure 3: Block diagram of the respiratory system model.

The equations describing the dynamics between the three compartments are given by:

$$\frac{dP_{aCO_2}(t)}{dt} = \frac{863\dot{Q}K_{CO_2}[P_{VCO_2}(t - \tau_v) - P_{aCO_2}(t)]}{M_{LCO_2}} + \frac{E_F\dot{V}_I[P_{ICO_2} - P_{aCO_2}(t)]}{M_{LCO_2}}, \quad (1)$$

$$\frac{dP_{aO_2}(t)}{dt} = \frac{863\dot{Q}[m_vP_{VO_2}(t - \tau_v) - m_aP_{aO_2}(t) + B_v - B_a]}{M_{LO_2}} + \frac{E_F\dot{V}_I[P_{IO_2} - P_{aO_2}(t)]}{M_{LO_2}}, \quad (2)$$

$$\frac{dP_{\text{BCO}_2}(t)}{dt} = \frac{MR_{\text{BCO}_2}}{M_{\text{BCO}_2} K_{\text{BCO}_2}} + \frac{[\dot{Q}_B(P_{\text{aCO}_2}(t - \tau_B) - P_{\text{BCO}_2}(t))]}{M_{\text{BCO}_2}}, \quad (3)$$

$$\frac{dP_{\text{VCO}_2}(t)}{dt} = \frac{MR_{\text{TCO}_2}}{M_{\text{TCO}_2} K_{\text{CO}_2}} + \frac{[\dot{Q}_T(P_{\text{aCO}_2}(t - \tau_T) - P_{\text{VCO}_2}(t))]}{M_{\text{TCO}_2}}, \quad (4)$$

$$\frac{dP_{\text{VO}_2}(t)}{dt} = \frac{\dot{Q}_T[m_a P_{\text{aO}_2}(t - \tau_T) - m_v P_{\text{VO}_2}(t) + B_a - B_v] - MR_{\text{TO}_2}}{M_{\text{TO}_2} m_v}. \quad (5)$$

Equations (1) and (2) describe the lung compartment partial pressures of CO_2 and O_2 respectively. Equations (4) and (5) describe the tissue compartment (including also brain tissue) partial pressures of CO_2 and O_2 respectively. Equation (3) describes the brain compartment CO_2 partial pressure. E_F , P_{IO_2} , K_{CO_2} , m_a , m_v , B_a and B_v are constants. The constants K_{CO_2} , m_a , m_v , B_a and B_v occur in the so-called dissociation laws relating gas concentrations to partial pressures. P_{IO_2} represents inspired oxygen. We include an alveolar arterial gradient of 4 mm Hg (unless otherwise indicated) by reducing P_{IO_2} by this amount [19]. The CO_2 dissociation law is assumed linear while the O_2 dissociation law is nonlinear but approximately piecewise linear. In the above model, it was assumed that the O_2 partial pressures stay within one band of the piecewise linear representation thus making it linear. Furthermore, the metabolic rates and compartment volumes are assumed constant. E_F reduces the effectiveness of ventilation and is used to model the effects of the ventilatory dead space. Ventilatory dead space refers to the fact that, on inspiration, one first brings into the alveoli air from the upper conducting airways (where no gas exchange occurs) left over from expiration. This air is fully equilibrated with the venous partial pressures of CO_2 and O_2 and hence does not contribute to the ventilation process. This dead space represents approximately 25 -30 % of the air moved during inspiration.

The ventilation rate \dot{V}_I depends on the signals sent from the peripheral and central sensors and the peripheral and central control effects are additive [3]. Thus

$$\dot{V}_I = \dot{V}_{\text{periph}} + \dot{V}_{\text{cent}}, \quad (6)$$

where

$$\begin{aligned} \dot{V}_{\text{cent}} &= \text{ventilation due to the central control signal,} \\ \dot{V}_{\text{periph}} &= \text{ventilation due to the peripheral control signal.} \end{aligned}$$

Physiologically, we do not assign any meaning to a negative \dot{V}_I , \dot{V}_{periph} or \dot{V}_{cent} . Let \dot{V}_P be the function defining ventilation due to the peripheral control signal

and \dot{V}_C be the function defining ventilation due to the central control signal. Then, we set \dot{V}_P and \dot{V}_C equal to zero should these functions become negative. Using the following notation

$$[[x]] = \begin{cases} x & \text{for } x \geq 0 \\ 0 & \text{for } x < 0 \end{cases}.$$

the control equation actually takes the form

$$\dot{V}_I = [[\dot{V}_P]] + [[\dot{V}_C]]$$

where

$$\dot{V}_P = G_P \exp(-0.05 P_{aO_2}(t - \tau_a))(P_{aCO_2}(t - \tau_a) - I_P)$$

and

$$\dot{V}_C = G_C(P_{BCO_2}(t) - \frac{MR_{BCO_2}}{K_{CO_2}\dot{Q}_B} - I_C).$$

Here, G_C and G_P are control gains and I_C and I_P are cutoff thresholds. However, to simplify our discussion, we will omit this notation while always maintaining that the peripheral and central ventilation rates will be greater than or equal to zero.

The control equation describing the rate of ventilation \dot{V}_I is thus [11]

$$\begin{aligned} \dot{V}_I = & G_P \exp(-0.05 P_{aO_2}(t - \tau_a))(P_{aCO_2}(t - \tau_a) - I_P) \\ & + G_C(P_{BCO_2}(t) - \frac{MR_{BCO_2}}{K_{CO_2}\dot{Q}_B} - I_C). \end{aligned} \quad (7)$$

The first term in (7) describes \dot{V}_{periph} and the second term describes \dot{V}_{cent} .

Controller function \dot{V}_I represents general ventilatory drive in liters/minute. Tidal volume or breath by breath simulation can be obtained by considering the details of a single breath. During inspiration the first segment of air is left-over exhaled air remaining in the dead space of the lungs (the branching tubes which do not exchange gases). This volume is approximately 150 ml for an adult. Infant anatomical dead space decreases from a maximum at birth during the first years [17]. Neither this air nor expired air provides the same volumes of CO_2 and O_2 compared to fresh air. Hence \dot{V}_I will be replaced in the state equations by \dot{V}_{eff} as follows. On the first segment of inspiration (until the stale air in the dead space has passed into the lungs) \dot{V}_{eff} should be a reduced level of \dot{V}_I . During the remaining segment of inspiration \dot{V}_{eff} should equal \dot{V}_I .

Finally during expiration \dot{V}_{eff} will again be a reduced level of \dot{V}_I . In practice, we alter the value of EF in the state equations for P_{aCO_2} and P_{aO_2} to reduce \dot{V}_I . Furthermore, M_{LCO_2} and M_{LO_2} are varied during inspiration and expiration depending on \dot{V}_I (see Khoo et al. [10] for details). The actual chemical drive in the model will be proportionally larger to force the flow of fresh air through the lung compartment during the fresh air phase of inspiration (a factor of about 2.5). A small alveolar-arterial oxygen gradient (A-a) O_2 is assumed to account for ventilation/perfusion mismatch and a residual R-L shunt in adults [14]. Breath by breath calculations can be found as:

$$V_{\text{tidal}} = t_I \dot{V}_I ,$$

where

t_I = time of inspiration (around 1.5 sec)

\dot{V}_I = inspiration drive in liters per minute

4 Simulations of Human Respiratory Physiology

Simulations of various conditions are carried out using appropriate parameter values chosen to reflect these conditions. We present here simulations of the adult steady state and congestive heart condition using the parameter values given in [11]. These parameters and initial conditions are found in the various tables in [1]. The delay times are calculated by integrating backward the blood flow rates until the volumes are reached for the arterial segments leading from the lung to the site of the sensory elements [1]. The values used for these volumes are found in [5]. Numerical solutions are obtained using SNDDELM, a code developed by Lo and Jackiewicz [12] for the numerical solution of systems of neutral delay differential equations with state-dependent delays using Adams predictor-corrector methods. We are indebted to the authors for allowing us to use this robust code to perform all simulations reported in this paper.

4.1 Normal Awake Adult Case

Figures 4-6 represent the steady state levels for the system variables in a normal adult awake case. The simulated values for partial pressures, tidal volume, and blood flow are consistent with the data presented in [14].

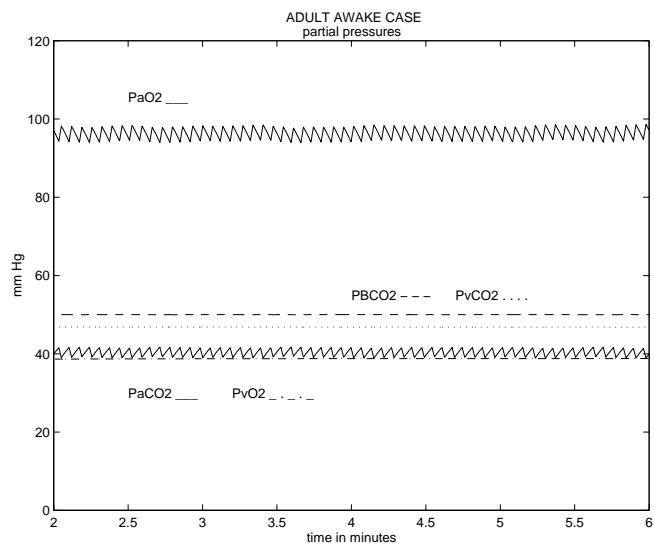


Figure 4: Partial pressure simulation values in normal adult awake case.

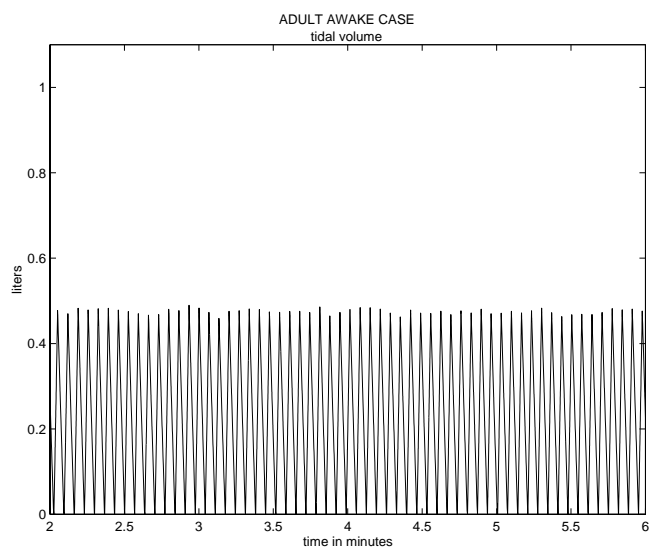


Figure 5: Tidal volume simulated result in normal adult awake case.

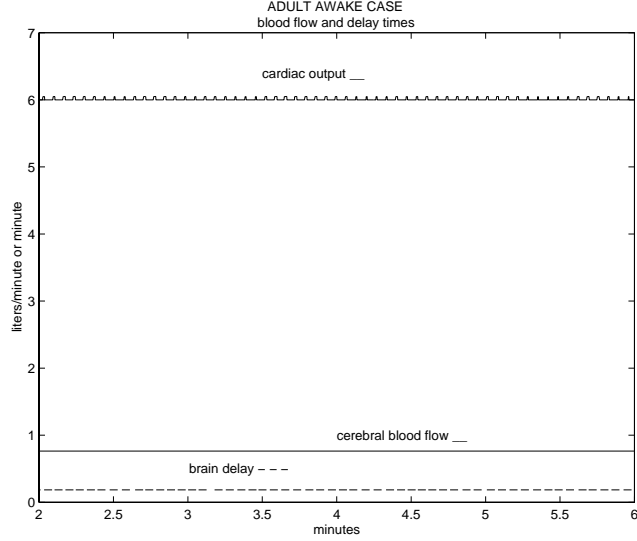


Figure 6: Blood flow simulated values in normal adult awake case.

4.2 Congestive Heart Condition

Figures 7-9 represent simulations using parameter values suggestive of the congestive heart condition. For this case, \dot{Q} is reduced to one half the normal level and hence the transport delays are doubled. This causes instability in the system resulting in central apnea (CA) and periodic breathing as can be seen in Figure 8. Cheyne-Stokes respiration (CSR) is exhibited. Early studies [7] suggested that excessive delay time might be the prime cause of (CSR). Current research suggests that a number of factors contribute to the phenomenon. For instance, it has been found that the application of continuous positive airway pressure (CPAP) acts to counter the onset of CSR [15]. Also, hypocapnia is an important factor in CSR in congestive heart failure and circulatory delay plays an important role in determining CSR-CA cycle length [16]. Excessive circulatory delay time certainly contributes to the “hunting phenomenon” first suggested by Douglas and Haldane to account for PB and CSR [8]. Simulations with the above model show that for certain values of controller gain, very long delay times may not produce oscillations but with other controller gain values such as used in the simulations in Figures 7-9 oscillations are produced.

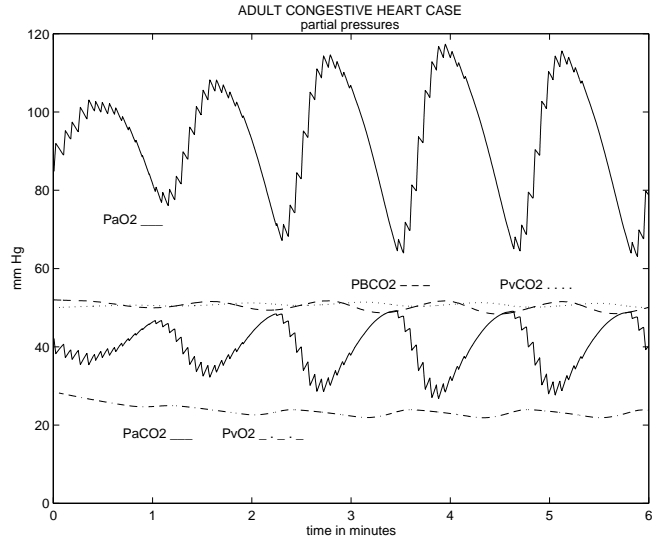


Figure 7: Partial pressure simulated values in an adult congestive heart case.

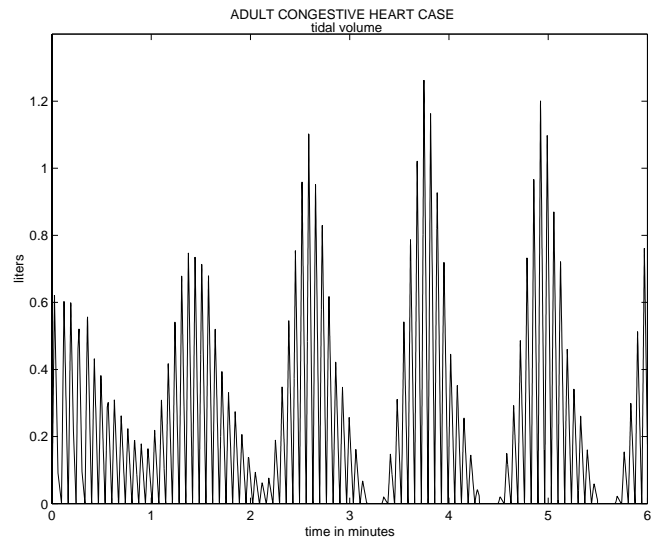


Figure 8: Tidal volume simulated result in an adult congestive heart case.

References

- [1] Batzel, J. and Tran, H. Modeling instability in the control system for

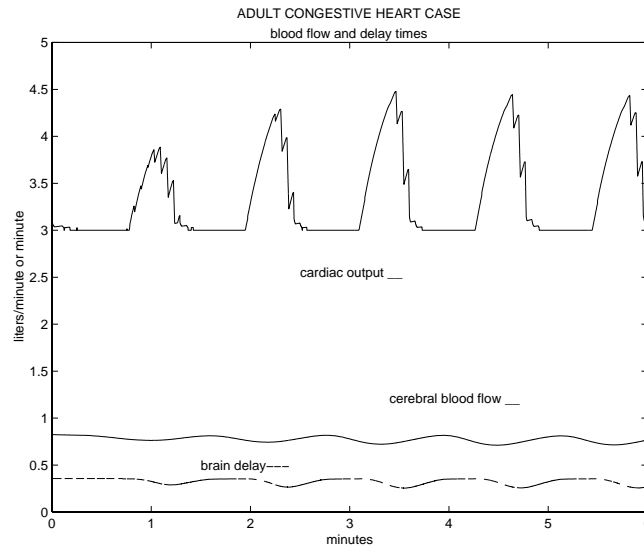


Figure 9: Blood flow simulated values in an adult congestive heart case.

human respiration: applications to infant non-REM sleep. *Applied Mathematics and Computation*, 110:1–51, 2000.

- [2] Cooke, K. and Grossman, Z. Discrete delay, distributed delay and stability switches. *J.Math.Analys.Appl.*, 86:592–627, 1982.
- [3] Cunningham, D.C, Robbins, P.A., and Wolff, C.B. Integration of respiratory responses. In Fishman A.P., editor, *Handbook of Physiology, The Respiratory System, Part II*, pages 475–528. American Physiol. Soc. Bethesda Md., 1986.
- [4] Douglas, C.G. and Haldane, J.S. Causes of PB or CSR. *J. Physiol. Lond.*, 38:401–419, 1909.
- [5] Grodins, F.S., Buell, J., and Bart, A.J. Mathematical analysis and digital simulation of the respiratory control system. *J. Appl. Physiology*, 22(2):260–276, 1967.
- [6] Guyton, A.C. *Physiology of the Human Body*. Saunders, Philadelphia, 1984.
- [7] Guyton, A.C., Crowell, J.W., and Moore, J.W. Basic oscillating mechanism of Cheyne-Stokes breathing. *Amer.J.Physiol.*, 187:395–398, 1956.

- [8] Khoo, M.C.K. Periodic breathing. In Grystal R. G. and West J.B. et al, editors, *The Lung: Scientific Foundations*, pages 1419–1431. Raven Press Ltd. New York, 1991.
- [9] Khoo, M.C.K. Periodic breathing. In R.G. Crystal and J.B. et al West, editors, *The Lung : Scientific Foundations*, pages 1851–1863. Lippincott-Raven N.Y., 1997.
- [10] Khoo, M.C.K. and Kronauer, R.E. Estimation of cardiopulmonary parameters for quasi-optimal inputs. *1983 Proc. 2nd Am. Control Conf.*, pages 46–51, 1983.
- [11] Khoo, M.C.K, Kronauer, R.E., Strohl, K.P., and Slutsky, A.S. Factors inducing periodic breathing in humans: a general model. *J. Appl. Physiol.*, 53(3):644–659, 1982.
- [12] Lo, E. and Jackiewicz, Z.(jackiewi@zjsun.la.asu.edu). SNDELLM code, 1992.
- [13] Longobardo, G.S., Cherniack, N.S., and Gothe, B. Factors affecting respiratory system stability. *Annal. Biomed. Eng.*, 17(4):377–396, 1989.
- [14] Mines, A.H. *Respiratory Physiology*. Raven Press, N.Y. N.Y., 1986.
- [15] Naughton, M.T., Benard, D.C., Rutherford, R., and Bradley, T.D. Effect of continuous positive airway pressure on central sleep apnea and nocturnal P_{CO_2} in heart failure. *Am.J.Respir.Crit.Care Med.*, 150(6 pt.1):1598–1604, 1994.
- [16] Naughton, M.T., Benard, D.C., Tam, A., Rutherford, R., and Bradley, T.D. Role of hyperventilation in the pathogenesis of central sleep apneas in patients with congestive heart failure. *Am-Rev-Respir-Dis.*, 148(2):330–338, 1993.
- [17] Numa, A.H. and Newth, C.J. Anatomical dead space in infants and children. *J. Appl. Physiol.*, 80(5):1485–1489, 1996.
- [18] Southall, D.P. Role of apnea in the Sudden Infant Death Syndrome. *Pediatrics*, 80(1):73–84, 1988.
- [19] West, J.B. *Respiratory Physiology*. Williams and Willaims Co., 1979.